Breakdown Voltage Measurements of Silicon Microstrip Detectors

Zelalem Asmamaw
Electrical Engineering
Brown University
Providence, RI 02912

August 10, 2001

Project Supervisor: Ronald Lipton

Abstract:

This project aims at providing an analysis of breakdown voltage values of silicon detectors for the D0 experiment. The measurements of voltage and response currents were made thought the development of LabVIEW programs and the assembly of various measurement apparatus circuitry. Through these means, alterations of breakdown voltage characteristics due to beryllium application, radiation, and structural differences in silicon detectors have been quantified.

Contents:

Introduction:

The underlying mission of the Fermi National Accelerator laboratory is to study the precise makeup and components of matter at the smallest scale. This quest for unveiling the fundamental particles of the universe is facilitated through the use of particle accelerators: counter-rotating beams of particles are brought to collision, crossing each other at specially designed detectors. One such detector at the Fermilab Tevatron ring is the D0, which was constructed to study proton-antiproton collisions with a center-of-mass energy of up to 1800GeV. At the heart of this large apparatus, depicted in Figure 1, is a tracking system composed of silicon detectors that record the trajectories of the high-energy particles produced in the collision. These silicon detectors are semiconductor devices with voltage applied across the p-n junction. (A sample silicon detector is presented in Figure 3.) Detailed properties of the silicon detectors will be presented in further sections, however, to be brief, the detectors comprise of minute pads with numerous silicon strips a fraction of a millimeter wide. Incident charged particles produce electron-hole pairs, which are separated by the resultant electric field and collected at electrodes. In turn, these charges generate electric signals that exactly indicate which strips the particles have traversed. The many layers of silicon allow physicists to determine the direction that the particles travel.

The objective of this investigation is to study the extent to which inter strip voltage can be applied before resulting in avalanche breakdown. The study explores the changes in breakdown voltage values among the strips in different types of silicon detectors. It also presents the effects of radiation and external substances on the detectors and how these factors result in a different set of data for breakdown voltage values. After examining the properties of silicon strip detectors and the role of radiation, this paper outlines the experimental procedure as well as measured data in the form of distribution plots and current-voltage graphs.

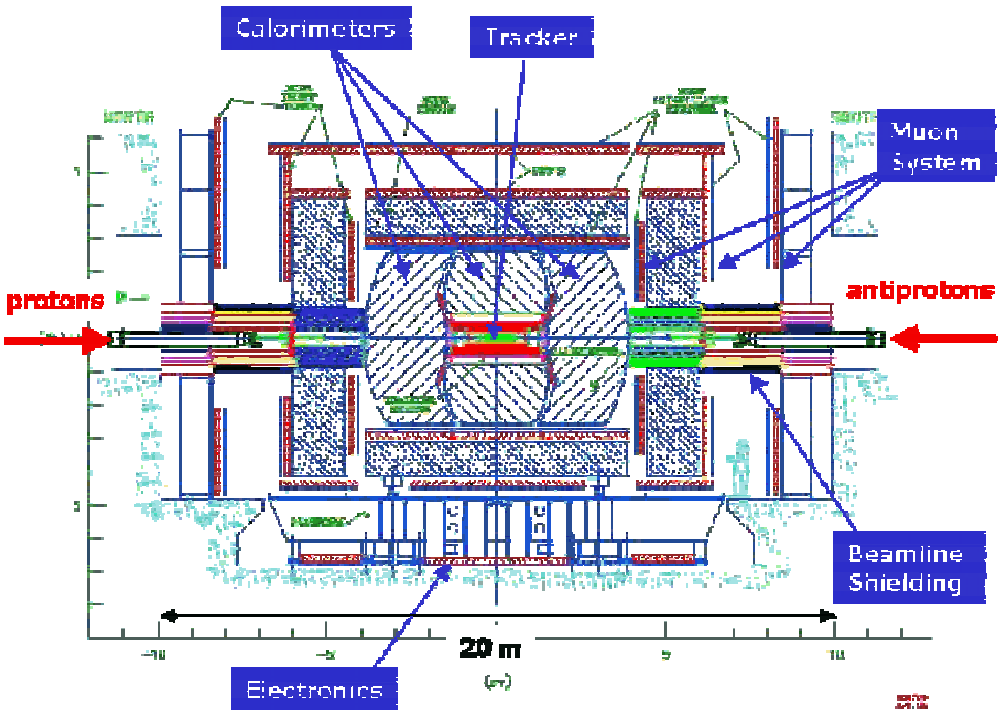

Figure 1: The D0 detector

Figure 2: Artistic interpretation of the D0 silicon tracker (the position of the tracker is depicted at the center of Figure 1)

Figure 3: A prototype F-disk silicon detector (these wedge shaped detectors are arranged to form parts of the silicon tracker shown in Figure 2)

Theory:

I. Charge Carriers in Intrinsic Semiconductors

Semiconductor particle detectors use silicon primarily in a single crystal formation. Each atom in the silicon face-centered cubic lattice is surrounded by its four nearest neighbor atoms, each with four valence electrons. Covalent bonding arises among the atoms from the quantum mechanical interactions between the shared electrons. At 0K, no free electrons are available for electrical conduction. However, at higher temperatures, the electrons can be thermally excited out of a covalent bond and become free to participate in electrical conduction. This leaves electron vacancies in the covalent bond referred to as "holes." The movement of holes also contributes to the electrical conductivity of the semiconductor material. The value of the conductivity, γ, is related to the charge carrier densities and their mobility as follows:

$$\gamma = q(\mu_e n_e + \mu_h n_h)$$

where μ_e, μ_h represent electron and hole mobility while n_e, n_h stand for electron and hole density. Externally triggered processes such as ionization and exposure to electromagnetic waves in the UV range use this property to alter the conductivity of semiconductors. For instance, photons with energies greater than the band gap energy of silicon can excite an electron into the conduction band, leaving a hole in the valence band. (Silicon has an energy gap of 1.11eV.) The ability of silicon to collect these created charges allows its use as a particle detector.

However, in order to use silicon as a particle detector, almost all the free charge carriers have to be removed from the silicon bulk. Consider the following illustration to clarify this concept: a strip like counter made of pure intrinsic silicon with 5cm length and 100μm width would contain $2.2*10^7$ free electron-hole pairs. (The unavoidable presence of impurities would increase this value.) After traversing such a detector, a minimum ionizing particle looses 116KeV of its energy resulting in a total signal of 32000 electron-hole pairs. The signal would thus be three orders of magnitude lower than the number of free carrier pairs. Hence, it would be too faint and completely

covered by the fluctuations of the detector current (which is referred to as leakage current). One method commonly used by modern particle detectors to remove free charge carries from the silicon bulk is the formation of a p-n diode structure.

II. The P-N Junction in Silicon Detectors

In addition to the thermally generated intrinsic carriers, it is possible to create carriers in semiconductors by introducing impurities into the crystal: a process referred to as doping. If the impurity atom belongs to group V of the periodic table, four of its valence electrons would be employed to form covalent bonds with the silicon atom, whilst the fifth valence electron contributes to the conductivity. This is accomplished as the donor impurity forms an energy level very near the conduction band in silicon, thereby enabling the electrons to enter the conduction band. This is an n-type material. On the other hand, dopants from column III would introduce impurity levels in silicon near the valence band. Even at low temperatures, enough thermal energy is available to excite electrons from the valence band into the impurity level, leaving behind holes in the valence band that would contribute to the conductivity. This is a p-type material.

If we brought p- and n- type semiconductor materials into contact to form a p-n junction, carrier diffusion occurs as holes from the p side diffuse into the n side, and electrons diffuse from n to p. This is illustrated in the following figure:

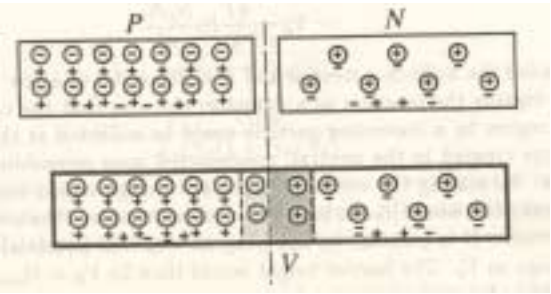

Figure 4: Formation of depletion region as two crystals of opposite types are brought together

This diffusion current, however, cannot build up indefinitely because an opposing electric field is created at the junction. To clarify, consider that electrons diffusing from n to p leave behind uncompensated donor ions (N_d^+) in the n material, and holes leaving the p region leave behind uncompensated acceptors (N_a^-). Thus, a region of positive space charge near the n side and negative charge near the p side would develop. Therefore, the

resulting electric field creates a drift component of current from n to p, opposing the diffusion current. The width of the region with no free charge carriers, known as the depletion region, can be determined with the following expression:

$$W = \left[\frac{2\varepsilon V_o}{q} \left(\frac{1}{N_a} + \frac{1}{N_d} \right) \right]^{1/2}$$

where ε, q are constants and N_a, N_d represent concentration of acceptors and donors. V_o stands for the potential difference that builds up between the n-type and p-type layers. This indicates that the width of the depletion region can be altered by applying external voltage across the junction. A positive voltage applied on the p-side and a negative one on the n-side (forward biasing) would oppose the built up internal voltage, as a result the depletion region would be reduced and the current between the terminals grows exponentially. Similarly, when negative voltage is applied on the p-side and positive voltage on the n-side (reverse biasing), the depletion region would grow. The effects of biasing on the resulting current from the junction is depicted below:

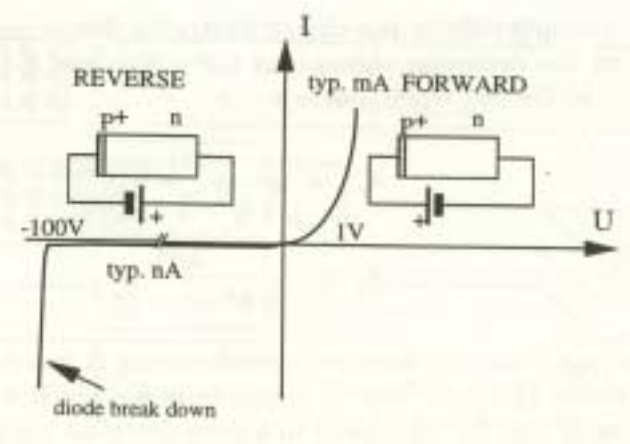

Figure 5: Current-voltage characteristics of a diode under forward and reverse biasing

The voltage necessary to extend the depletion region over an entire detector is calculated as follows:

$$V_{fd} = \frac{qN_d T^2}{2\varepsilon}$$

where T is the thickness of the detector. As stated earlier, the application of silicon as a particle detector depends upon the presence of a minimum number of free charge carriers, which is tantamount to a maximum depletion region. Hence, this can be achieved by applying the necessary voltage to a reverse biased p-n junction. In fact, in order to avoid

losses in charge collection, the silicon detectors are overbiased. There is, however, one key limiting factor to applying maximum reverse bias voltage: the breakdown phenomenon.

III. Avalanche Breakdown:

An important mechanism for the occurrence of breakdown is avalanche multiplication or the impact ionization of host atoms by carriers in high electric field. To illustrate this phenomenon, imagine that the electric field in the depletion region is large enough so that an electron entering from the p side may be accelerated to high enough kinetic energy to cause an ionizing collision with the silicon/dopant crystal lattice. As a result of this interaction, the original electron and the generated electron would both be swept to the n side, while the generated hole would be swept to the p side. On their paths, however, the resulting carriers also have the chance of creating a new electron-hole pair, and each of those can also create an electron-hole pair, and so forth.

To approximate the degree of carrier multiplication, assume that a carrier of either type has a probability P of having an ionizing collision and that there are n_{in} number of electrons entering from the p side. This will give us the total number of electrons out of the region at n after many collisions:

$$n_{out} = n_{in}(1 + P + P^2 + P^3 + ...)$$

The electron multiplication factor, M_n, is defined as the ratio of n_{in} to n_{out}:

$$M_n = \frac{n_{out}}{n_{in}} = 1 + P + P^2 + P^3 + ... = \frac{1}{1-P}$$

Physically, we would expect the ionization probability to increase with the applied voltage. Measurements of carrier multiplication support this prediction by an empirical relation:

$$M = \frac{1}{1 - \left(V / V_{br} \right)^n}$$

where V_{br} is the breakdown voltage: the critical voltage at which point the reverse current through the junction increases sharply, and relatively large currents can flow with

little further increase in voltage. The value for the breakdown voltage can be further quantified through the following expression:

$$V_{br} = \frac{\varepsilon E_c^2}{2qN}$$

Here, N represents the effective carrier concentration and E_c is the electric potential of the coupling aluminization. (The coupling alumization and other components of silicon microstrip detectors are explained in the following section.)

IV. Design of Silicon Strip Detectors

The position localization accuracy of silicon detectors is achieved by dividing the p-n diode into fine parallel strips that act as individual independent electrodes. The figure below shows a schematic cross-section of a strip detector:

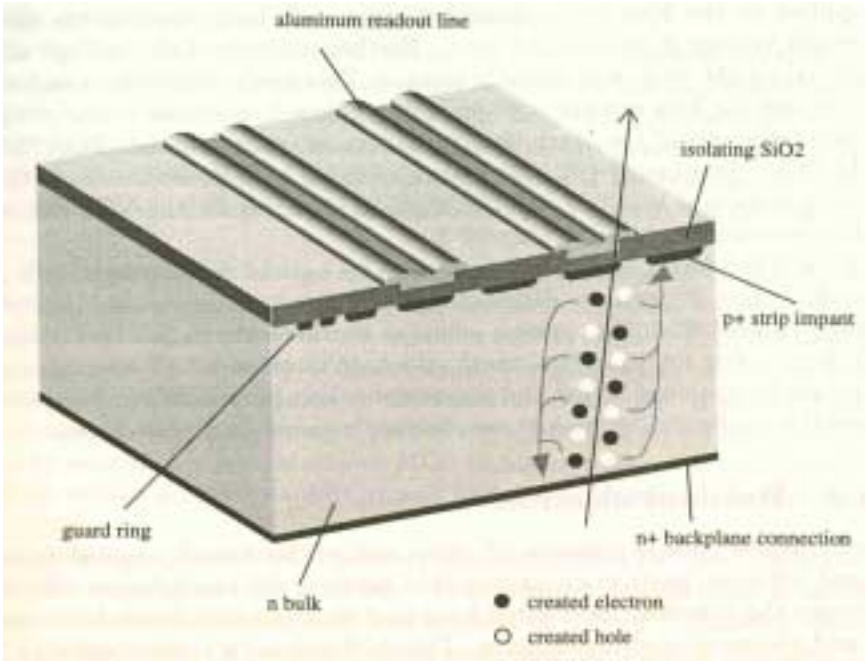

Figure 6: Schematic layout of a silicon strip detector

When an incident particle ionizes the n bulk, the resulting holes and electrons drift towards the p+ (cathode) and n+ (anode) sides due to the electric field caused by the depletion voltage. Consequently, these collected charges produce a current pulse on the electrodes, which are individually read out by amplifiers. Thereby, the position of the strip at which the signal was generated yields the position of the traversing particle.

The n bulk serves as the detection volume, while the n+ backplane connection is used as an ohmic contact to the n type material. (The "+" sign indicates that the material has high concentration of dopants—above $10^{20}cm^3$.) The p+ implant is used to deplete the n bulk and acts as a measuring electrode. The aluminum readout line serves as a contact to the input of an amplifier (referred to as a DC coupling contact). However, there would be a problem here because when the aluminum line is in direct ohmic contact with the strip implant, the constant detector leakage current would flow into the amplifier. This can result in serious operation problems by saturating the charge amplifier. Thus, a silicon dioxide insulating layer is placed between the aluminum metal layer and the p+ implants. The capacitance formed by the strip implant, the SiO_2, and the readout line (known as the coupling capacitance) enables the signal current to be induced in the readout line.

A "bias line" present at the edge of the detector connects the individual strips through individual resistors to a fixed potential. The resistance for these bias resistors has to be high enough to separate the strips from one anther. The resistor values also have to be constant since large variations in resistor values can lead to variations in the applied strip depletion voltage. Furthermore, the detector is enclosed by "guard ring(s)". The guard ring is used to define the active depletion region and to prevent the leakage current from being absorbed by the edge strips, which would depreciate their performance.

V. Effects of Radiation

High doses of irradiation can alter the detection properties of a detector in two main ways: surface damage in the oxide layer (a result of long term ionization) and bulk damage (which is caused by displacements). Long term ionization effect is a multi-step process. As noted earlier, some of the electron-hole pairs produced by ionizing particles recombine while most drift away, which either end up in "traps" or escape from the silicon dioxide layer. The carriers that are trapped on levels with low ionization energies are thermally excited into the conduction (electrons) or valence (holes) band. In the energy gap, new silicon dioxide interface levels are induced (which are practically

permanent). The main effect of induced charges in the oxide is the change of the electric field in the silicon detector.

The displacement process begins when an incident particle hits an atom in the silicon lattice and transfers enough energy to displace it. This leads to what is known as the Frenkel defect: the occurrence of interstitials and vacancies. The fragments of the displaced atom induce further displacements. This alteration in the doping concentration results in changes of internal electric field, capacitance and resistivity, losses in charge collection, and increase in leakage current. The change in leakage current, ΔI, is parametrized by

$$\Delta I = \alpha \phi V$$

where α is the damage constant (approximately $3*10^{17} A/cm^3$), ϕ is the fluence (the flux normalized to 1MeV of neutrons), and V is the active volume of the detector.

Experimental Details:

I. Electronic Devices

In order to measure the leakage current and, thereby, evaluate the breakdown voltage for the individual strips of silicon detectors, this project has employed some electronic devices. Voltage is supplied to the detectors by a Keithley 237 source measure unit. The Keithley 237 can apply voltage while measuring the current response of the detector, or vise versa. It can deliver a potential difference across its terminals in the range of –1100V to 1100V. It has measurement capability for current between 10fA to 100mA when providing source voltage in the range of ±110V, whereas it can measure current at ±10mA maximum when the source voltage is in the ±1100V range. One useful feature of the Keithley 237 is the compliance facility that is installed to protect the circuitry of the sample that is being tested. This is accomplished, when applying a voltage source, by setting the compliance limit, which sets the maximum current output level. Another important feature is its filtering function, which averages the results (it allows 2, 4, 8, 16, or 32 readings to be averaged).

The Keithley 237 measures current of the entire detector, so in order to measure individual strip currents, a Keithley 485 autoranging picoammeter is incorporated in the

system. The Keithley 485 provides 100fA sensitivity. It measures DC current on seven ranges covering 10 decades from 100fA to 2mA.

During the tests, the silicon detector is placed on a Rucker & Kolls Model 680A Semi-Automatic Wafer Prober (RK 680A). A special probe placed on the chuck stage of the RK 680A is put into contact with the DC test pad (or the aluminum contact points) provided on the silicon detector. This probe is connected to the input of the Keithley 485 to provide strip current measurements. The chuck stage of the RK 680A allows the vertical (Z-axis) movement of the probe, while the roller bearing stage and the leadscrew drives enable accurate X- and Y-axes positioning of the silicon wafer. The Theta Drive assemblies provide a means to align the detector with respect to the probe. Furthermore, the microscope support allows viewing of the detector components with a 6:1 zoom ratio.

II. Connection of Measuring Devices to Detector

The testing devices have to be integrated with the detector in specific ways in order to make accurate measurements. Two setups have been constructed during this project: one for connection to the DC test pads and another for connection with the aluminum contact points. The following schematic represents the testing system for the DC test pad connection:

(Note: Several components of the silicon detector are not displayed. Figure not drawn to scale.)

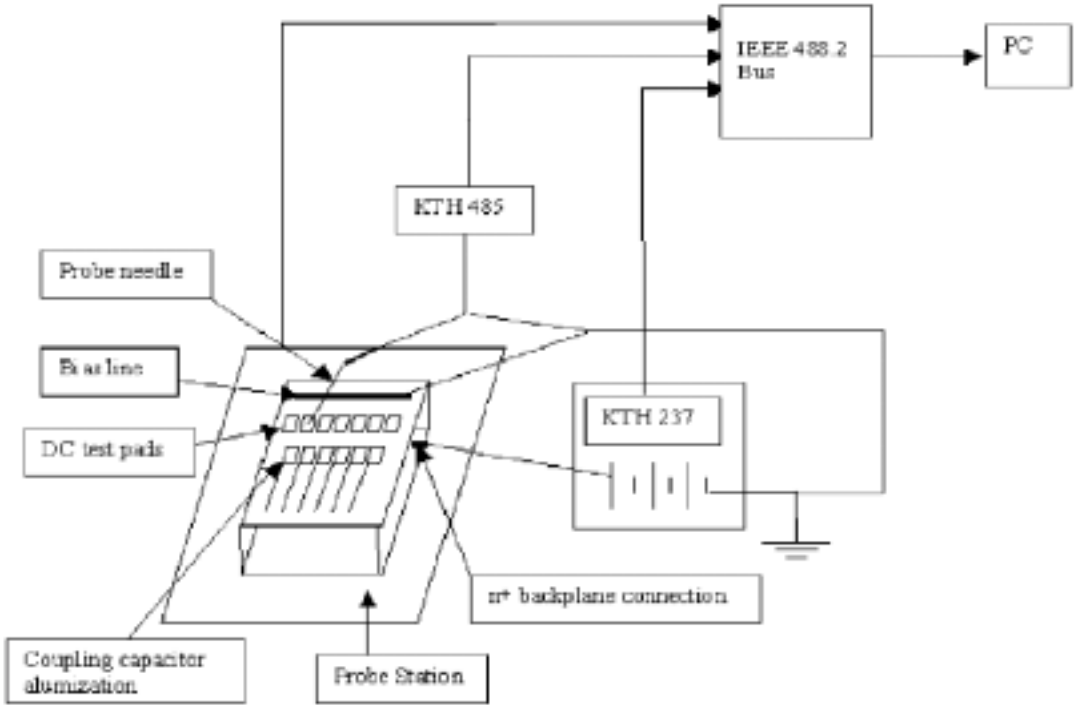

Figure 7: Schematic for DC test pad connection

The schematic below illustrates the setup for the aluminization contact test:

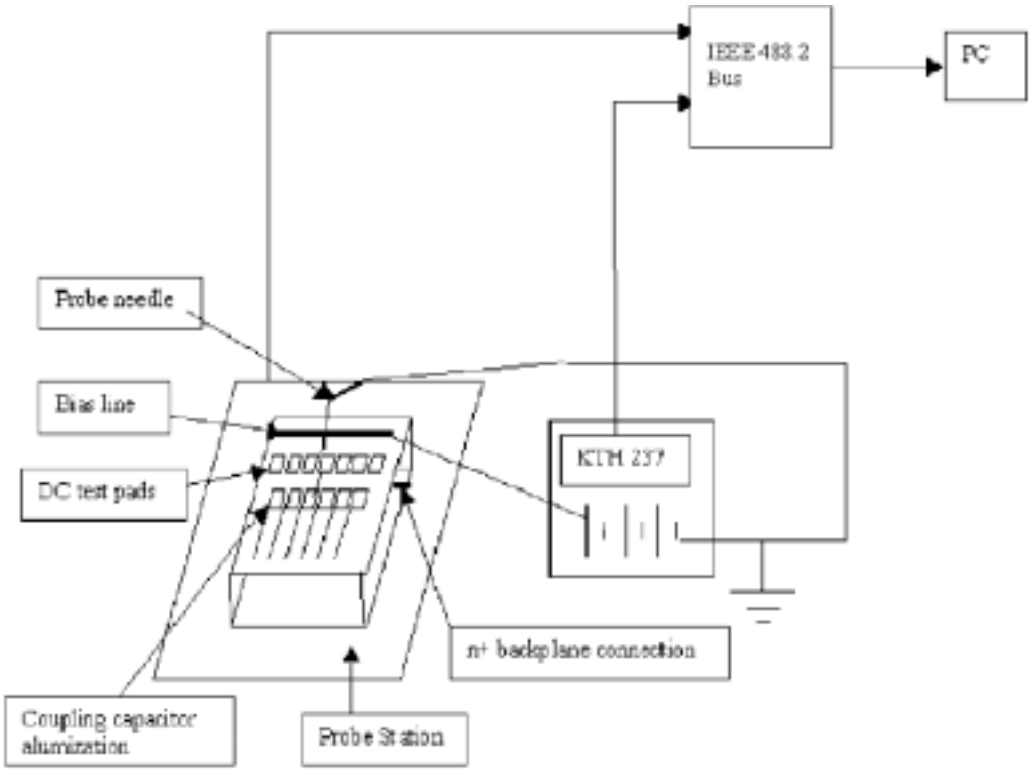

Figure 8: Schematic for aluminum metal layer connection

The differences between this setup and the former one are (1) the probe needle is in contact with the coupling capacitor aluminization instead of the DC test pad, (2) the Keithley 485 is not incorporated, (3) the positive terminal of the Keithley 237 voltage output is connected to the bias line instead of the n+ backplane connection, and (4) the negative terminal of the voltage output is connected to the probe.

III. Virtual Instruments

As depicted in the last two schematics, all the devices are linked to an IEEE 488.2 bus, which is one type of a General Purpose Interface Bus (GPIB). The GPIB carries two types of messages from the PC: device-dependent and interface messages. The device-dependent messages contain device-specific instructions such as programming commands, measurement results, and machine status. The interface messages, on the other hand, perform actions such as addressing/unaddressing devices, initializing the bus, and setting device modes for remote programming. The PC defines and transmits these

messages through LabVIEW programs, known as virtual instruments (VIs), that are created by a graphical programming language, G. The VIs consist of an interactive user interface (the 'front panel') which simulates the panel of a physical instrument, a data flow diagram (or the 'block diagram') that serves as the source code, and icon connections that allow VIs to pass data to a subVI (a VI within another VI).

For this project, a higher level VI, the 'RK 680A controller' VI, was modified to call on other VIs that performed more specific tasks. (Sample VI source codes have been presented in the appendix section for illustrative purposes.) This VI, additionally, had the capacity to input the specific dimensions or parameters of different types of detectors such as the distance between the test pads in a given row, the distance between the first pad of the first row and the first pad of the second row, the number of channels in the detector, and so forth. Furthermore, a starting voltage for measurement, a final voltage, voltage increments, address of file to save these data, and the GPIB address of devices to collect these data from can all be specified from this VI. Through the definition of such values, the chuck stage of the RK 680A probe station moves the probe needle from one test pad to another on a detector while measuring the current response as the Keithley 237 increments the supply voltage according to the specifications. The 'RK 680A controller' VI presents a number of subroutines in the form of sequence structures. Through these functions, this VI can initialize the probe station, align the detector with respect to the needle, move the detector to a 'loading' or 'home' positions (each programmable), and call VIs to make current, capacitance, resistance, or voltage measurements. The current/voltage measurement calls initialize the instrument drivers for the Keithley 237 and 485. These drivers are used to configure the devices, arm their triggering systems, transfer data to or from the instruments, perform operations such as calibration or storage and recall of setups, and finally terminate the software connection to instruments and free up system resources.

Results and Discussion:

Through the creation, modification, and utilization of the various hardware and software described above, this project has managed to garner numerous interstrip current-voltage data to analyze the breakdown values for silicon detectors. The resulting data is

presented primarily in two fashions. One is a plot of current versus voltage for a few selected channels or strips on a single detector. This is used simply to give an idea of the overall pattern of change in the current response as a result of increasing voltage application on silicon strips of different kinds. The second is a distribution plot presenting the current response (Y-axis) of all the strips for a given voltage. This is more important since it reveals the degree of uniformity of all the strips. Even though distribution plots have been made at different voltages per detector, for the sake of brevity, in this paper, the plots are for voltages that are fairly close to the breakdown value.

The generated data can be used for three main reasons: to compare two types of detectors, to note the effects of radiation, and to determine the changes resulting from the application of external substances (beryllium) on the detectors. (Note: unless otherwise stated, assume DC test pad connections.)

I. Comparison of F-Disk with Elma Detectors

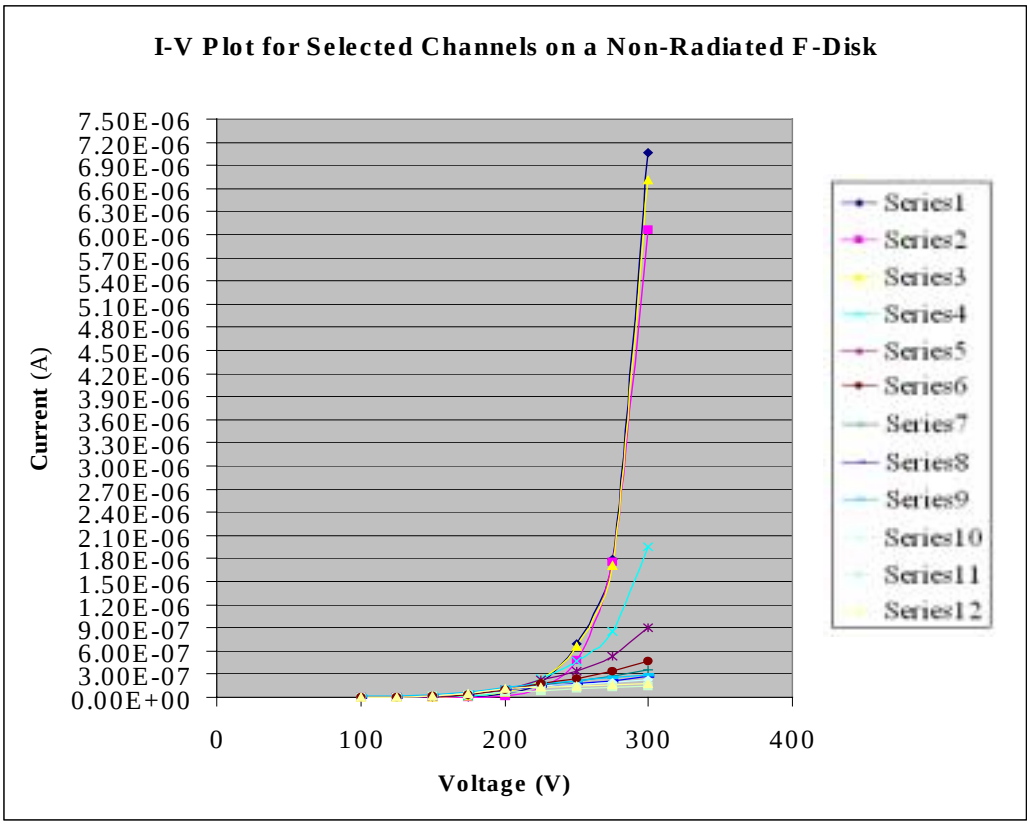

Graph 1

From the above graph, we can see that the breakdown occurs near 250 volts. The following is a distribution plot at this value:

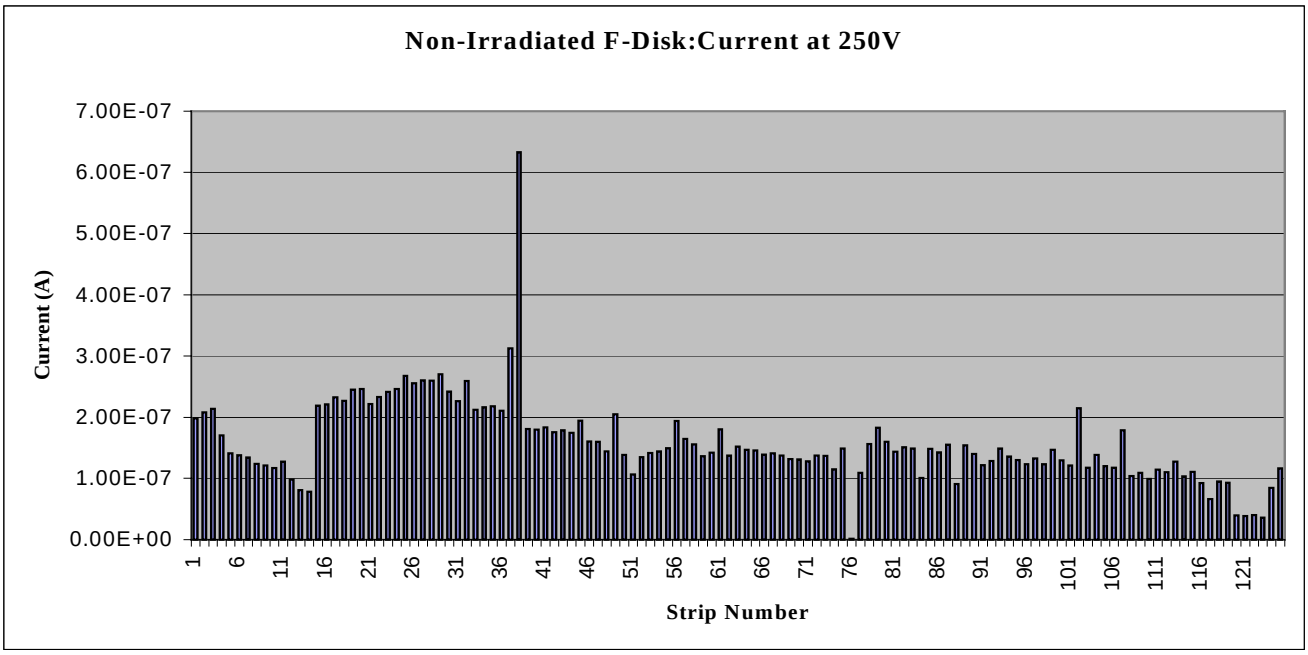

Graph 2

These results from a sample F-Disk can be compared to those generated from a prototype elma detector (elma 2-1-3):

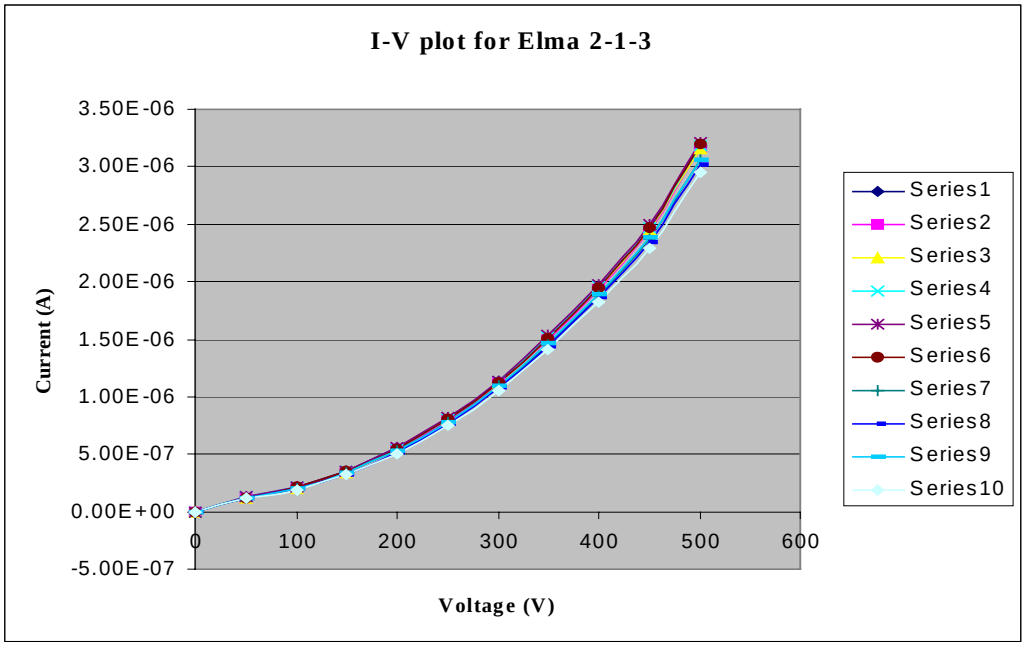

Graph 3

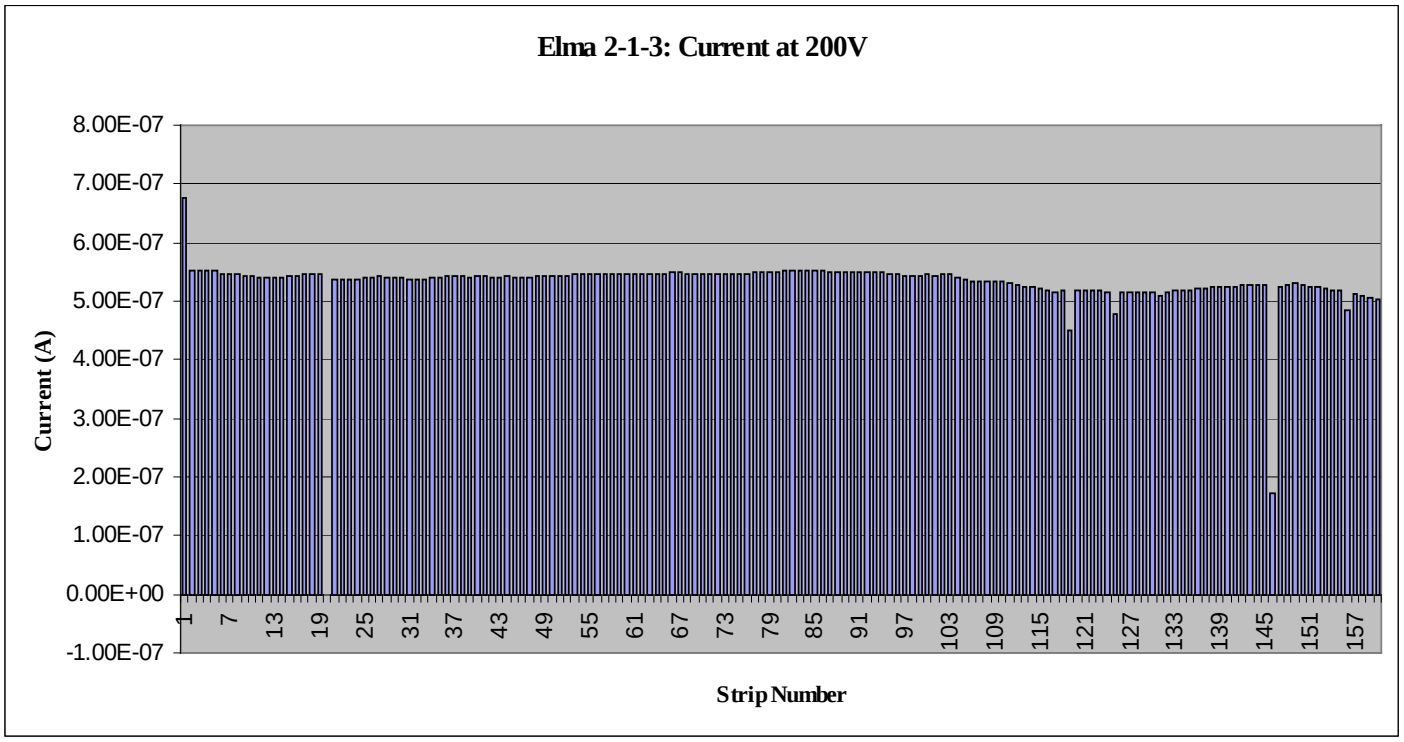

Graph 4

Clearly, we can see that the elma specimen has greater uniformity in strip current responses than the F-disk. The wedge shape of the F-disk implies that the strip have uneven length. Consequently, the number of electron hole pairs generated would not be equal, which indicates that the current would not be the same among the strips. Another factor for the difference between the two detectors is that in addition to SiO_2, the elma detectors have silicon nitride between the aluminimun metal layer and the p+ implants. This apparently improves the insulation.

II. Comparison with Irradiated Detectors

The data presented below was collected after making the aluminum contact lines connection. It was for two elma detectors: 2-1-3 and 2-1-4, the latter is the irradiated one. This serves not only as a way of observing the effects of radiation but also purely to assess breakdown values at the aluminization points.

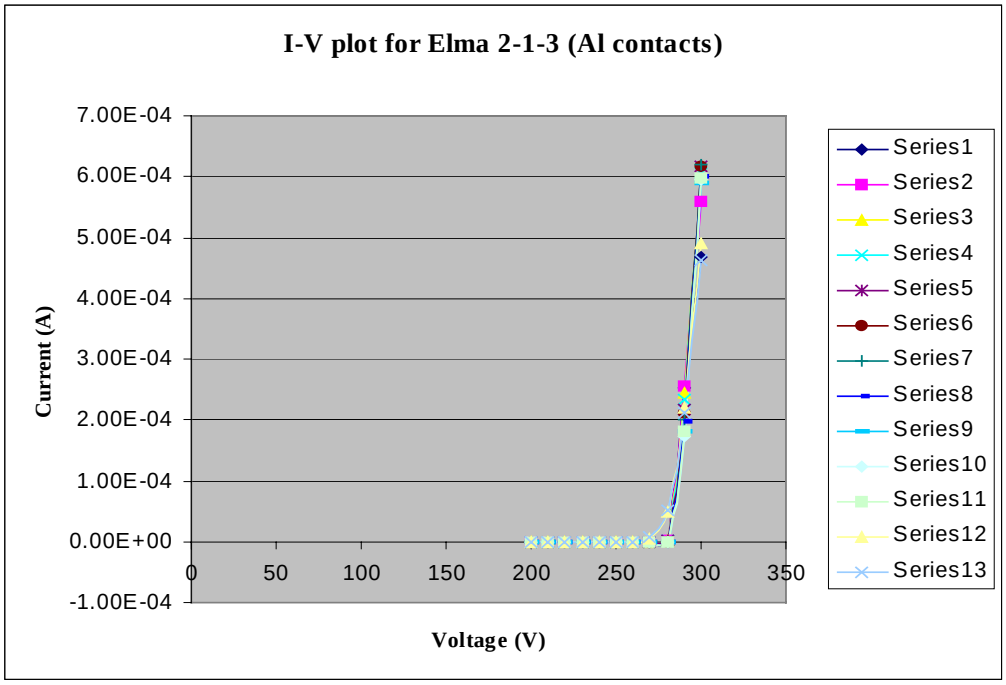

Graph 5

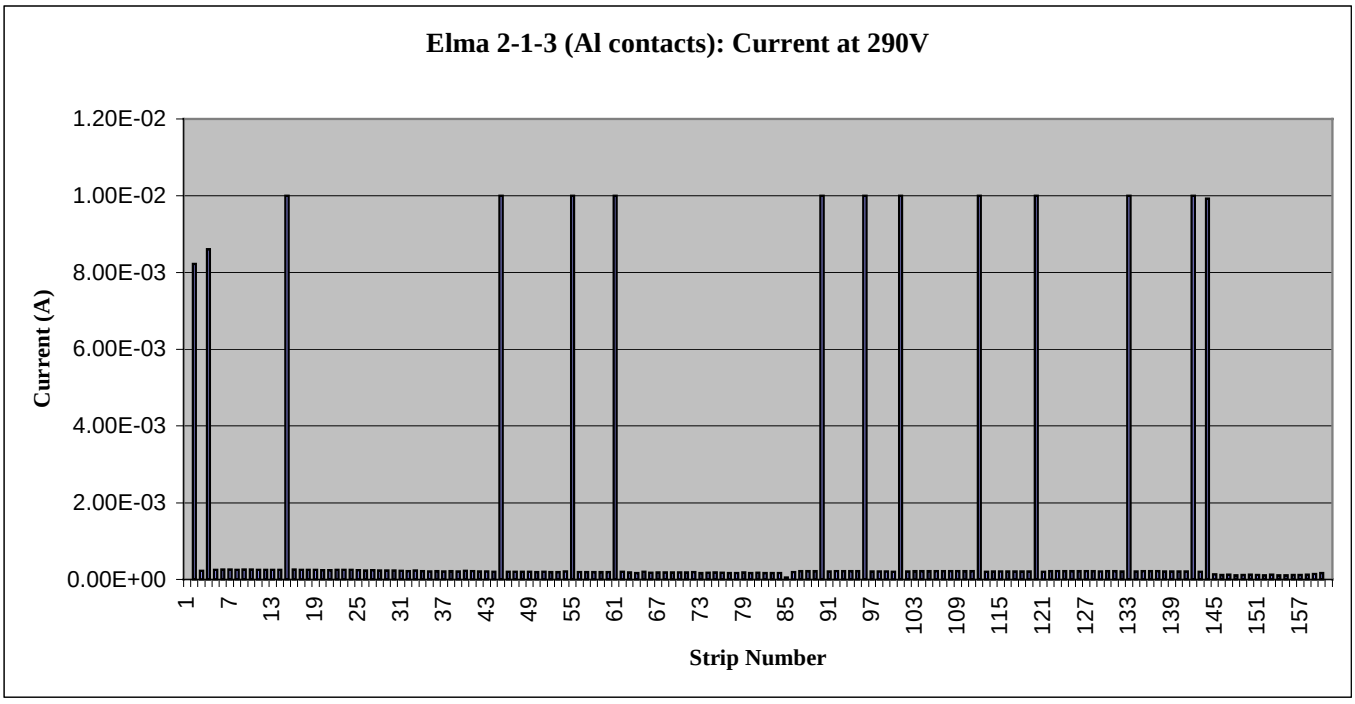

Graph 6

The elongated spikes that are seen in the above plot can be attributed to a limited number of strips that break exceptionally early resulting in, comparatively, a very high leakage current at the given voltage. The data above can be compared to that from a detector of identical composition (elma 2-1-4) that has been exposed to radiation dose rate of 0.4 mrem/hr.

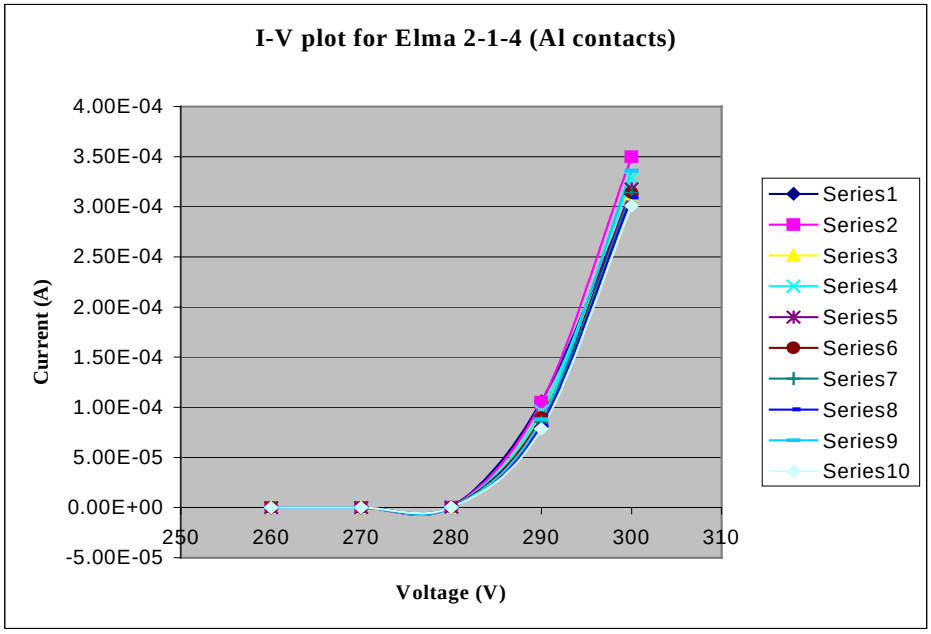

Graph 7

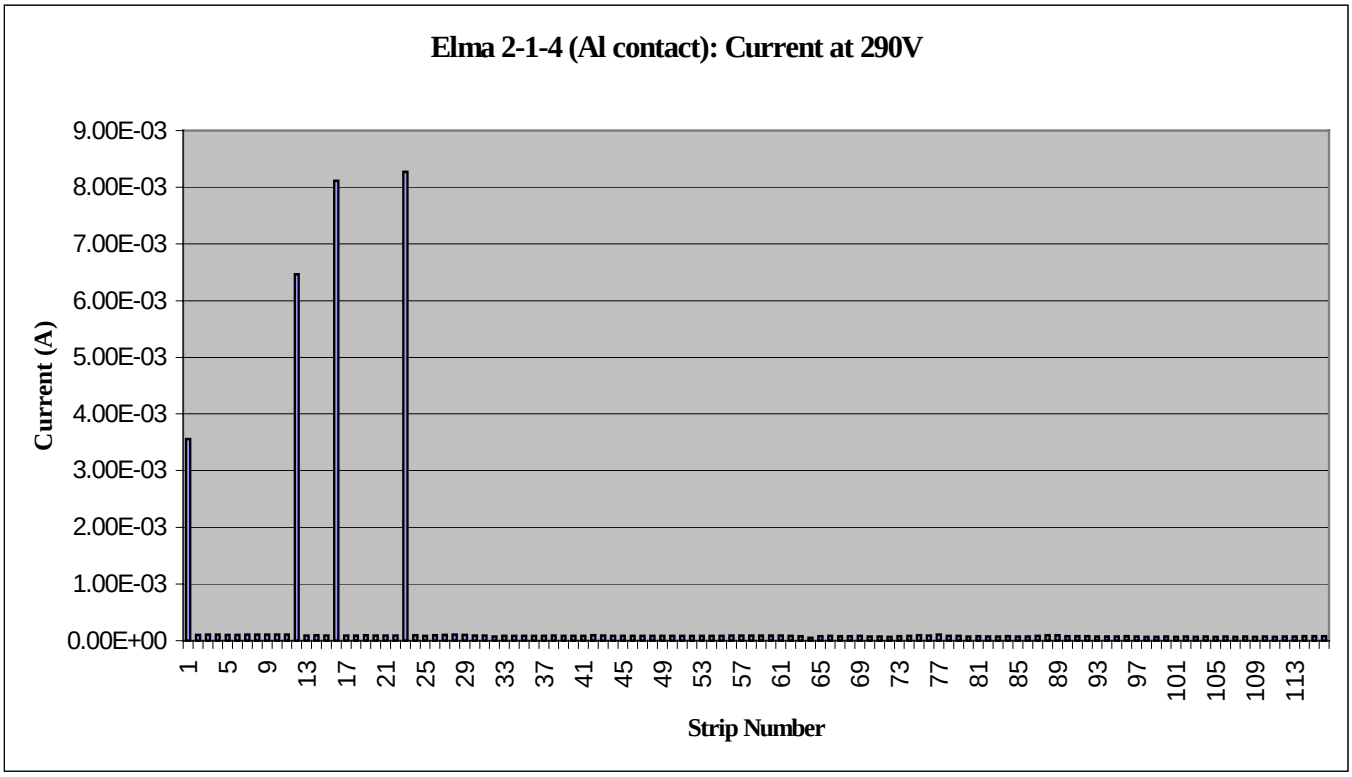

Graph 8

Thus, the I-V plots for the irradiated detector are smoother than that for the non-irradiated one. In other words, breakdown occurs gradually for the irradiated detector.

Furthermore, upon close examination, the distribution plot reveals that elma 2-1-4 has

less spikes and is more uniform. One reason for these occurrences is that as a result of radiation, the newly formed charge carriers would engulf the silicon bulk, thereby making the effects of preexisting free carriers less noticeable. Hence, the distribution plots are more consistent.

III. Comparison with Glued or Beryllium-Attached Detectors

In order to save space, research is underway to place the readout electronics for silicon detectors on top of the strips rather than at the end (as shown in figure3). The choice for Beryllium lies is due to the realization that the interaction with beams is proportional to the atomic number squared, and Be has the low atomic number of 4.

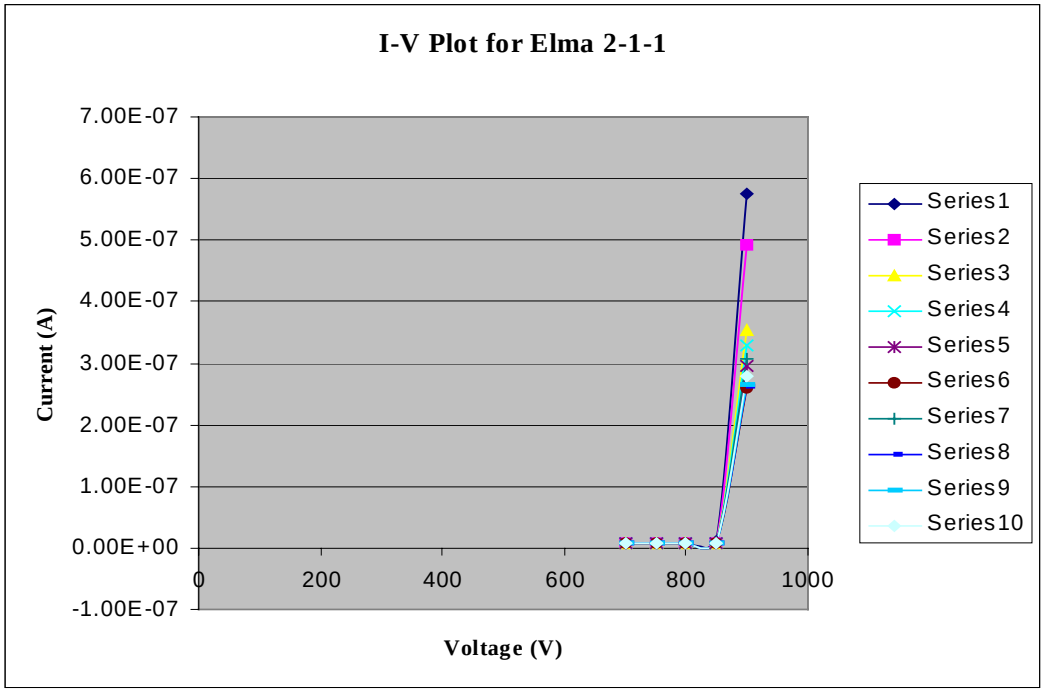

Graph 9

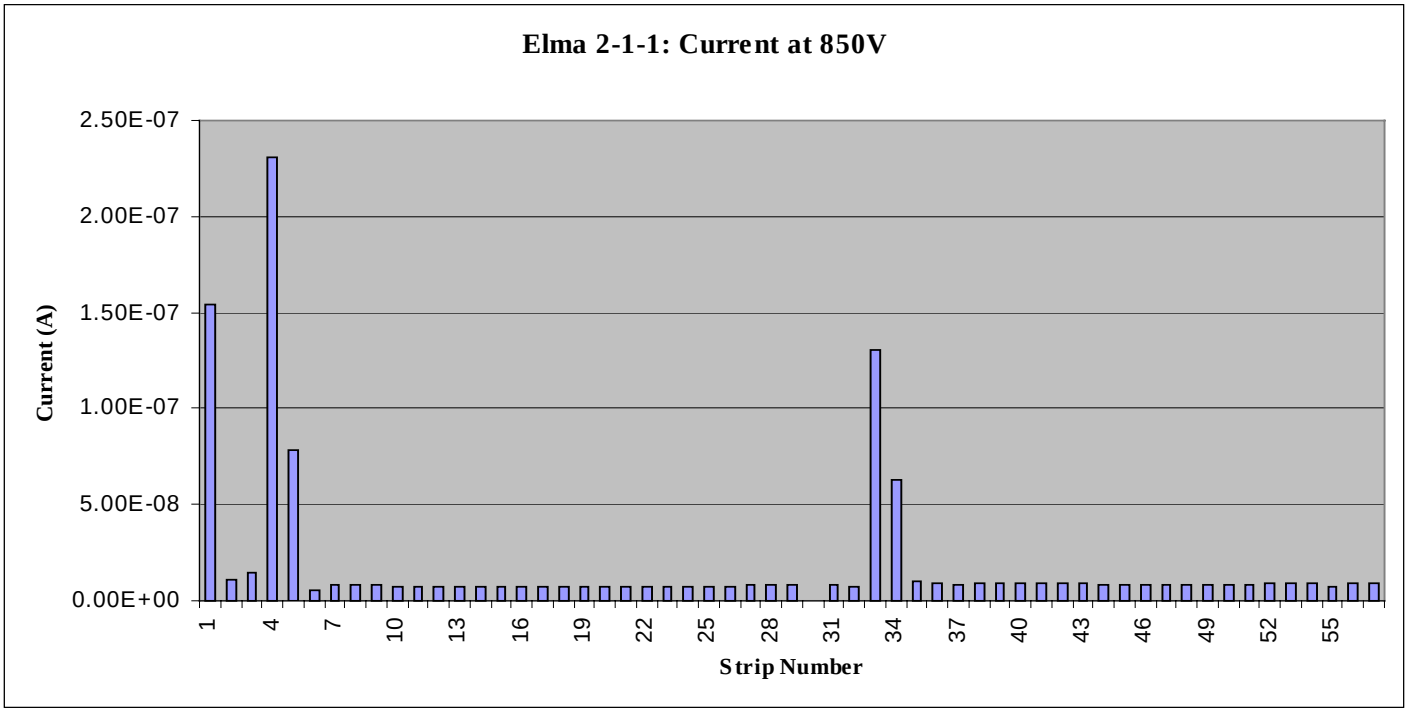

Graph 10

Below is the data retrieved after Beryllium was glued to some of the strips on elma 2-1-1:

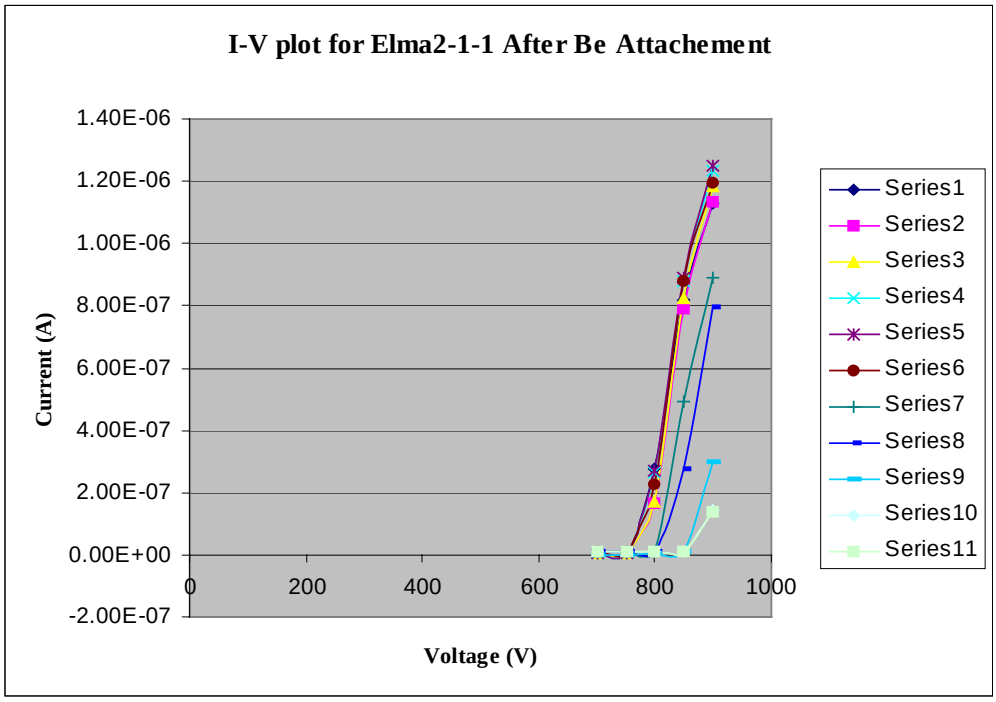

Graph 11

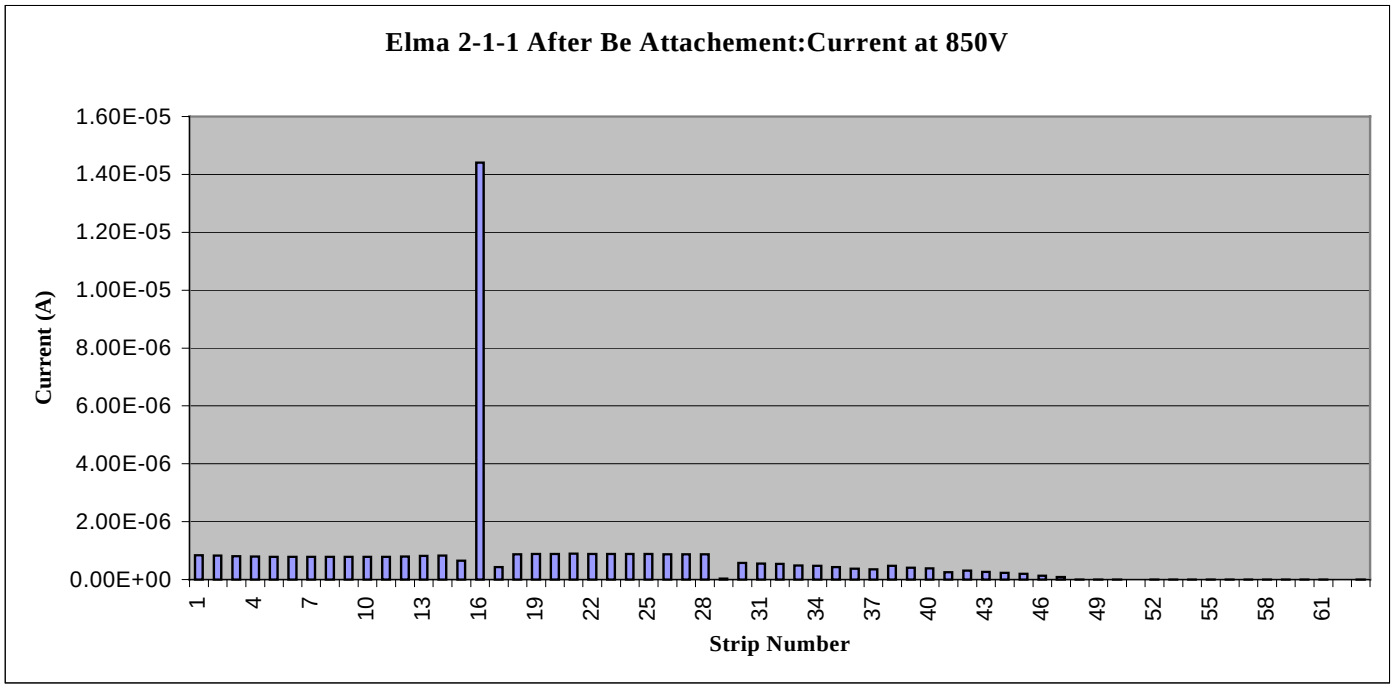

Graph 12

The plots show that the current responses are higher at any given voltage for the strips that were brought to contact with the beryllium. In other words, the breakdown voltage for these strips was lower than its original value. One cause for this observation is that some charge carriers are trapped at the points of application of such external substances, resulting in increased electric field around those areas. The measurements clearly indicate that the interaction between the glued beryllium and the silicon strips enhances the generation of electron-hole pairs.

Conclusion:

The objective of the project has been accomplished. The LabVIEW programs that were developed were able to accurately control the movements of the devices in addition to performing the necessary data acquisition. The experimental set-up made the current and voltage measurements to a reasonable accuracy. The accuracy of the data and the conclusions that can be drawn from these, however, are limited by some potential sources of error. These limitations include the effects of testing temperature (particularly for the irradiated detectors), cleanliness (removal of unwanted impurity from the detector surface), and slight exposure to light during testing. Hence, the conclusions that can be

made are to be done in light of these possible shortcomings. All in all, however, the changes in breakdown characteristics as a result of gluing, radiation, and different geometry or structural compositions of detectors that have been observed by this project all support the theoretical predictions.

References:

(1) Bock, R. K. and A. Vasilescu. "The Particle Detector Brief Book." March 1999. Cern. <http://rkb.home.cern.ch/rkb/titleD.html>.

(2) Jones, Michael Angus Scott. "Measurement of Depletion Voltage and Leakage Current for Silicon Strip Detectors." Dissertation. University of Manchester, September 1997.

(3) LabVIEW™ User Manual, Part Number 320999B-01. Austin, Texas: National Instruments Corporation, January 1998.

(4) Lipton, Ronald. "Silicon Detectors – Outline." March 2000. FermiLab . <http://www-ppd.fnal.gov/epp_www/Academic_Lectures/new_sil_lect.pdf>.

(5) Pernegger, Heinz. "The Silicon Ministrip Detector of the Delphi Very Forward Tracker." Dissertation. Hephy Vienna, February 1996.

(6) Sauli, Fabio. *Instrumentation in High Energy Physics*. Singapore: World Scientific Publishing Co. Pte. Ltd., 1992.

(7) Streetman, Ben G. *Solid State Electronic Devices*. New Jersey: Prentice Hall, 1990.

Acknowledgment:

I would like to thank the SIST committee members for giving me the opportunity to participate in this research. I would also like to give my gratitude to my supervisor, Ronald Lipton, for his guidance and advice on the testing of silicon detectors. Furthermore, special thanks to Steve Jakubowski and Matt Siegler from the Silicon Detector Group for their help on some practical tasks during the set-up of the testing system. Finally, I would like to recognize the SIST interns for making my summer experience enjoyable.

Appendix: LabVIEW Codes for Device Control

Note: These are only two of the several VIs that have been modified and created during the course of this project. The front panels are included merely for illustration but the block diagrams are intended for individuals who are familiar with the G programming language.

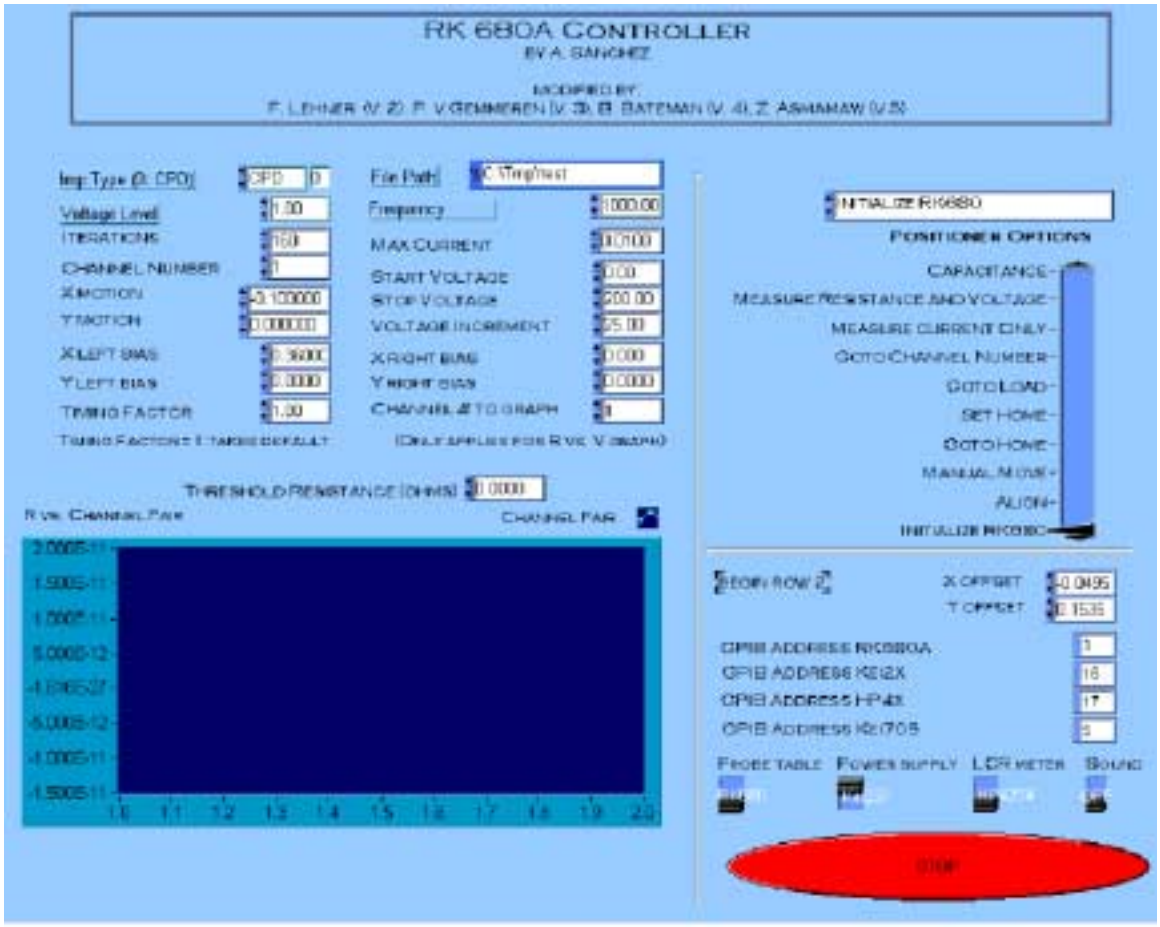

Figure 9: Front panel of the RK 680A Controller VI

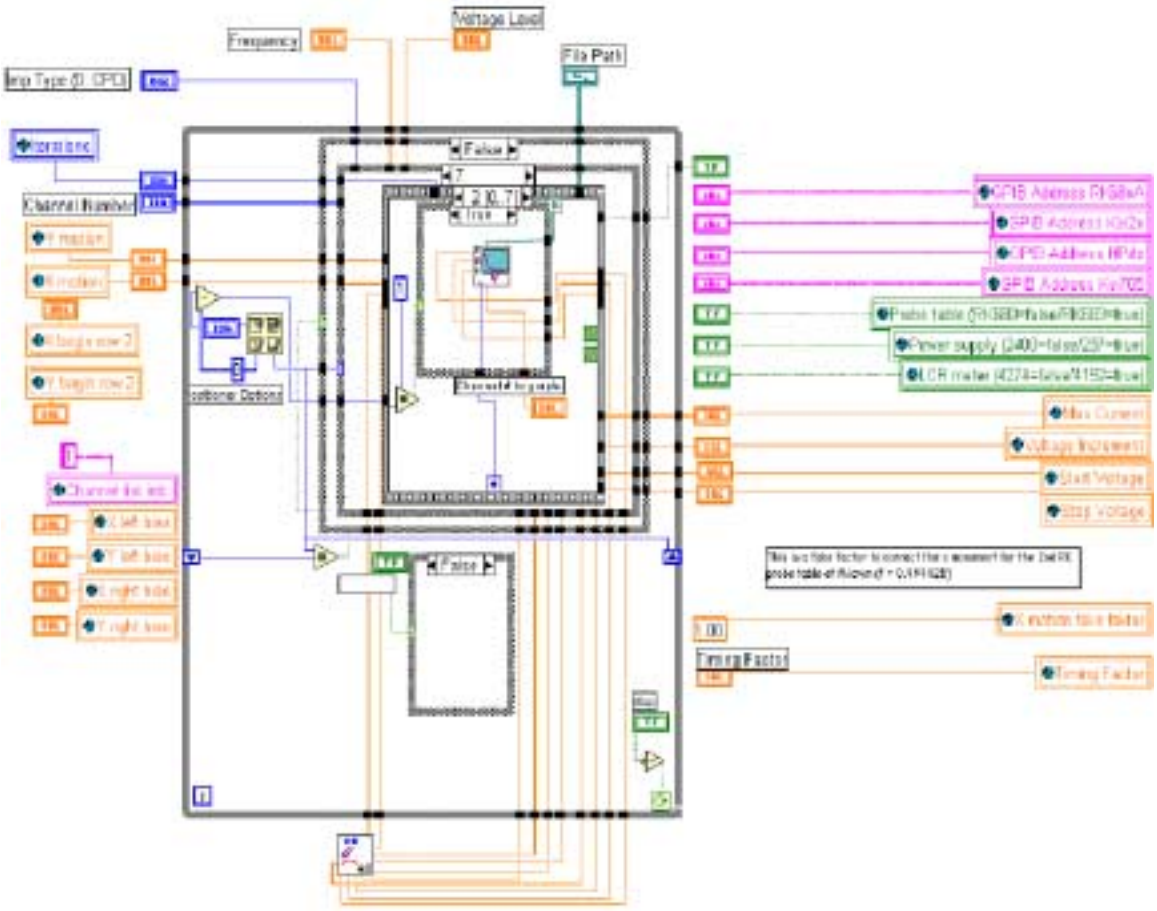

Figure 10: Block diagram for the RK 680A Controller VI

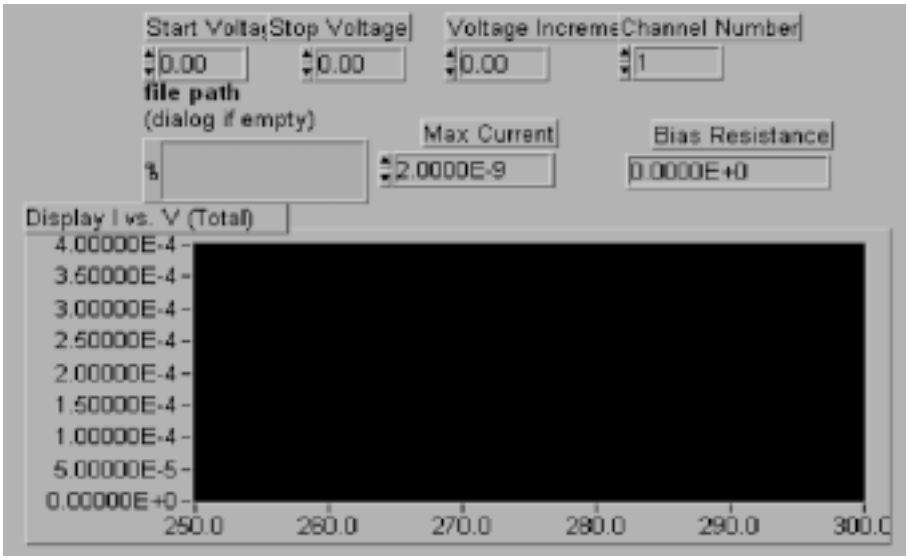

Figure 11: Front panel of the IV scan VI. (This VI saves the generated data to file and makes current-voltage plots.)

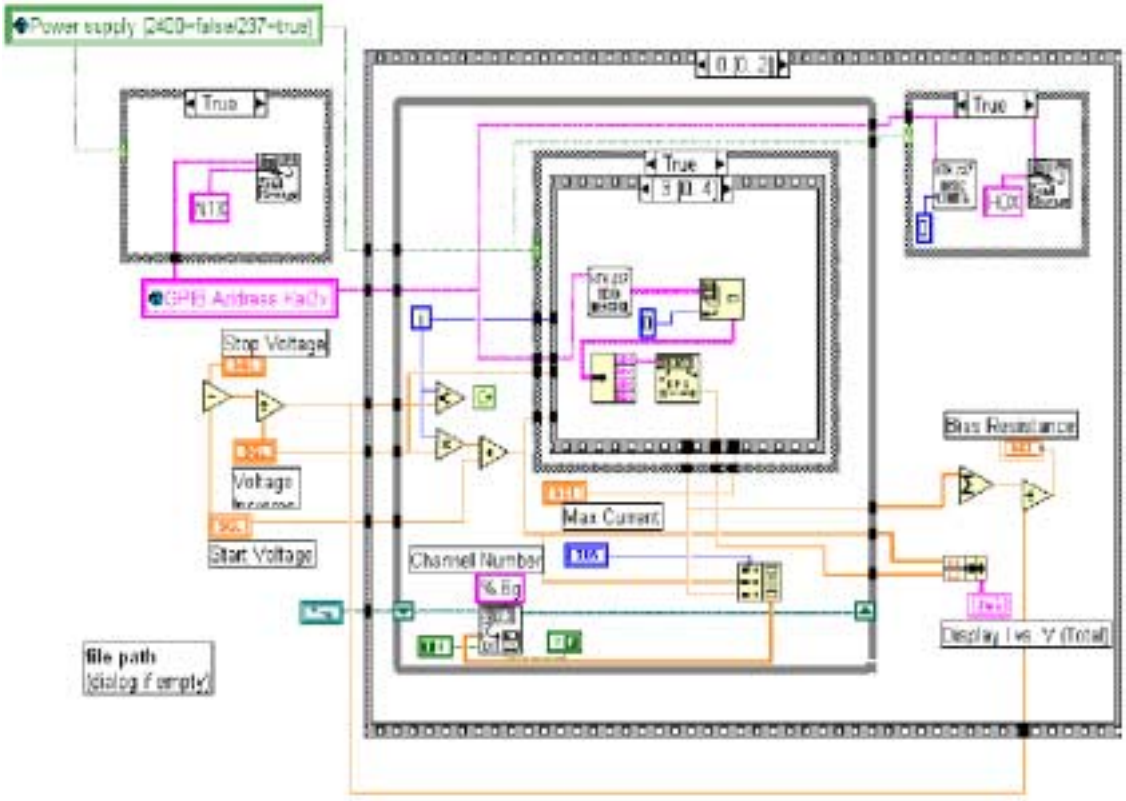

Figure 12: Block diagram of the IV scan VI.